

Electronic Supplementary Information

A facile “bottom-up” approach to free-standing nano-films based on manganese coordination clusters

Lei Zhang,^a Camelia I. Onet,^a Rodolphe Clérac,^{b,c} Mathieu Rouzières^{b,c}

Bartosz Marzec,^a Markus Boese,^d Munuswamy Venkatesan,^d and

Wolfgang Schmitt*^a

^a School of Chemistry & CRANN, University of Dublin, Trinity College, Dublin 2, Ireland. Tel: (+) 353-1-896-3495

^b CNRS, CRPP, UPR 8641, F-33600 Pessac, France.

^c Univ. Bordeaux, CRPP, UPR 8641, F-33600 Pessac, France.

^d School of Physics & CRANN, University of Dublin, Trinity College, Dublin 2, Ireland.

E-mail: schmittw@tcd.ie

Experimental Section

Materials and Instrumentation. Commercially available reagents were bought from Sigma-Aldrich and used as received without further purification. Fourier transform infrared spectroscopy (FTIR) data were collected on a PerkinElmer Spectrum 100 FT-IR Spectrometer. Elemental analyses (C, H, and N) were obtained from Microanalysis Lab, School of Chemistry & Chemical Biology, University College Dublin. Electrospray Ionization (ESI) mass spectra were collected using a TOF-MS (Time-of-Flight-Mass Spectrometry, LCT Premier) instrument supplied by Waters Corp. The electron microscopy studies of the films were carried out using a Carl Zeiss Ultra-Scanning Electron Microscope, a Zeiss Orion Plus-Helium Ion Microscope and a FEI Titan-transmission Electron Microscope.

Synthesis of $[(\text{Mn}^{\text{II}}_{0.5}\text{Mn}^{\text{III}}_{0.5})\text{Mn}^{\text{III}}_{12}(\mu_4\text{-O})_6(\mu\text{-OH})_2(\mu\text{-CH}_3\text{O})_4(\text{tert-butyl-PO}_3)_{10}(\text{CH}_3\text{OH})_6]\text{Cl}_{0.5}\cdot 6\text{CH}_3\text{OH}$ ($[\mathbf{1}]\text{Cl}_{0.5}\cdot 6\text{CH}_3\text{OH}$): (**Method A**) A mixture of $\text{MnCl}_2\cdot 4\text{H}_2\text{O}$ (0.039 g, 0.2 mmol), KMnO_4 (0.007 g, 0.04 mmol), *tert*-butylphosphonic acid (0.028 g, 0.2 mmol), Et_3N (0.06 ml) and CH_3OH (20 ml) was stirred at room temperature for 5 h. The resultant solution was filtered and the filtrate was kept at room temperature. Red crystals of $[\mathbf{1}]\text{Cl}_{0.5}\cdot 6\text{CH}_3\text{OH}$ were obtained within several weeks. Yield: 38% (based on Mn). CHN analysis on dried sample expected for $[\mathbf{1}]\text{Cl}_{0.5}\cdot 2\text{CH}_3\text{OH}$ ($\text{Mn}_{13}\text{P}_{10}\text{O}_{50}\text{C}_{52}\text{H}_{136}\text{Cl}_{0.5}$): calcd. (found) C 23.99 (23.34), H 5.27 (4.96)%. (**Method B**) A small amount of samples of $[(\text{Mn}^{\text{II}}_{0.5}\text{Mn}^{\text{III}}_{0.5})\text{Mn}^{\text{III}}_{12}(\mu_4\text{-O})_6(\mu\text{-OH})_2(\mu\text{-CH}_3\text{O})_4(\text{CH}_3\text{OH})_2(\text{tert-butyl-PO}_3)_{10}(4,4\text{-TDP})_2]\text{Cl}_{0.5}\cdot 8\text{CH}_3\text{OH}^{\text{SI}}$ were dissolved in MeOH during heating. The obtained solution was then cooled to room temperature. Red crystals of $[\mathbf{1}]\text{Cl}_{0.5}\cdot 6\text{CH}_3\text{OH}$ were obtained after several weeks.

Ref S1: L. Zhang, R. Clérac, C. I. Onet, M. Venkatesan, P. Heijboer and W. Schmitt, *Chem. Eur. J.*, 2012, **18**, 13984.

Synthesis of $[(\text{Mn}^{\text{II}}_{0.5}\text{Mn}^{\text{III}}_{0.5})\text{Mn}^{\text{III}}_{12}(\mu_4\text{-O})_6(\mu\text{-OH})_2(\mu\text{-CH}_3\text{O})_4(\text{tert-butyl-PO}_3)_{10}(\text{CH}_3\text{OH})_2(\text{Cl}_2)(\text{ppp})_2]\cdot 1.5(\text{H}_3\text{O})\cdot 8\text{CH}_3\text{OH}$ ([2]·1.5(H₃O)·8CH₃OH): A mixture of MnCl₂·4H₂O (0.102 g, 0.5 mmol), KMnO₄ (0.015 g, 0.1 mmol), *tert*-butylphosphonic acid (0.069 g, 0.5 mmol), 4-(3-phenylpropyl)-pyridine (0.10 ml) and CH₃OH (20 ml) was stirred at room temperature for 5 h. The resultant solution was filtered and the filtrate was kept at room temperature. Red crystals of [2]·1.5(H₃O)·8CH₃OH were obtained within several weeks. Yield: 41% (based on Mn). CHN analysis on dried sample expected for [2]·1.5(H₃O)·3CH₃OH (Mn₁₃P₁₀O_{48.5}N₂C₇₇H_{158.5}Cl₂): calcd. (found) C 31.00 (32.11), H 5.35 (5.81), N 0.94 (0.83)%.

X-ray Crystallography. Single crystal X-ray structure determination of [1]Cl_{0.5}·6CH₃OH and [2]·1.5(H₃O)·8CH₃OH was performed at 150(K) on the Bruker SMART Apex diffractometer using graphite-monochromated Mo-K α radiation. Absorption corrections were applied using SADABS.^{S2} Structures were solved by direct method and refined by full-matrix least-squares on F² using *SHELXTL*.^{S3} Crystal data and details of data collection and refinement were summarized in Table S1.

Crystallographic data, CCDC 907073, 907074 can be obtained free of charge from the Cambridge Crystallographic Data Centre via www.ccdc.cam.ac.uk/data_request/cif.

Ref S2: Sheldrick, G. M. *SADABS, Program for area detector adsorption correction*. Institute for Inorganic Chemistry, University of Göttingen, Göttingen (Germany), **1996**.

Ref S3: Sheldrick, G. M. *SHELXL-97, Program for solution of crystal structures*. University of Göttingen, Göttingen (Germany), **1997**.

Table S1. Crystal Data and Structure Refinements for [1]Cl_{0.5}·6CH₃OH and [2]·1.5(H₃O)·8CH₃OH.

	[1]Cl _{0.5} ·6CH ₃ OH	[2]·1.5(H ₃ O)·8CH ₃ OH
CCDC No	907073	907074
Crystal. determ. formula	C ₅₆ H ₁₅₂ Cl _{0.5} Mn ₁₃ O ₅₄ P ₁₀	C ₈₅ H _{178.5} Cl ₂ Mn ₁₃ N ₂ O _{53.5} P ₁₀
<i>Mr</i>	2731.42	3143.59
crystal system	triclinic	triclinic
space group	<i>P</i> -1	<i>P</i> -1
<i>a</i> [Å]	15.339(3)	15.005(3)
<i>b</i> [Å]	15.385(3)	16.396(3)
<i>c</i> [Å]	15.538(3)	16.397(3)
α [°]	116.11(3)	99.63(3)
β [°]	115.59(3)	110.20(3)
γ [°]	95.97(3)	114.28(3)
<i>V</i> [Å ³]	2767.2(19)	3217.6(20)
<i>Z</i>	1	1
<i>T</i> [K]	150(2)	150(2)
ρ_c [gcm ⁻³]	1.639	1.622
μ [mm ⁻¹]	1.669	1.478
reflns coll.	13713	11343
unique reflns	10396	9435
GOF	1.072	1.032
<i>R</i> 1[<i>I</i> > 2 σ (<i>I</i>)] ^[a]	0.0535	0.0445
<i>wR</i> 2[<i>I</i> > 2 σ (<i>I</i>)] ^[b]	0.1356	0.1184

[a] $R1 = \sum ||F_o| - |F_c|| / \sum |F_o|$.

[b] $wR2 = \{ \sum [w(F_o^2 - F_c^2)^2] / \sum [w(F_o^2)^2] \}^{1/2}$.

Table S2. Bond valence sum calculations for clusters **1** and **2**.

1	Mn site	Mn1	Mn2	Mn3	Mn4	Mn5	Mn6	Mn7
	BVS	2.696	3.167	3.131	3.180	3.148	3.148	3.098
	assigned O.S.	+3/+2	+3	+3	+3	+3	+3	+3
	OH/O²⁻ site	O1	O2	O3	O14			
	BVS	2.343	2.248	2.366	1.253			
	assigned O.S.	-2	-2	-2	-1			
2	Mn site	Mn1	Mn2	Mn3	Mn4	Mn5	Mn6	Mn7
	BVS	2.605	3.166	3.186	3.021	3.132	3.108	3.255
	assigned O.S.	+3/+2	+3	+3	+3	+3	+3	+3
	OH/O²⁻ site	O1	O2	O3	O20			
	BVS	2.360	2.348	2.041	1.238			
	assigned O.S.	-2	-2	-2	-1			

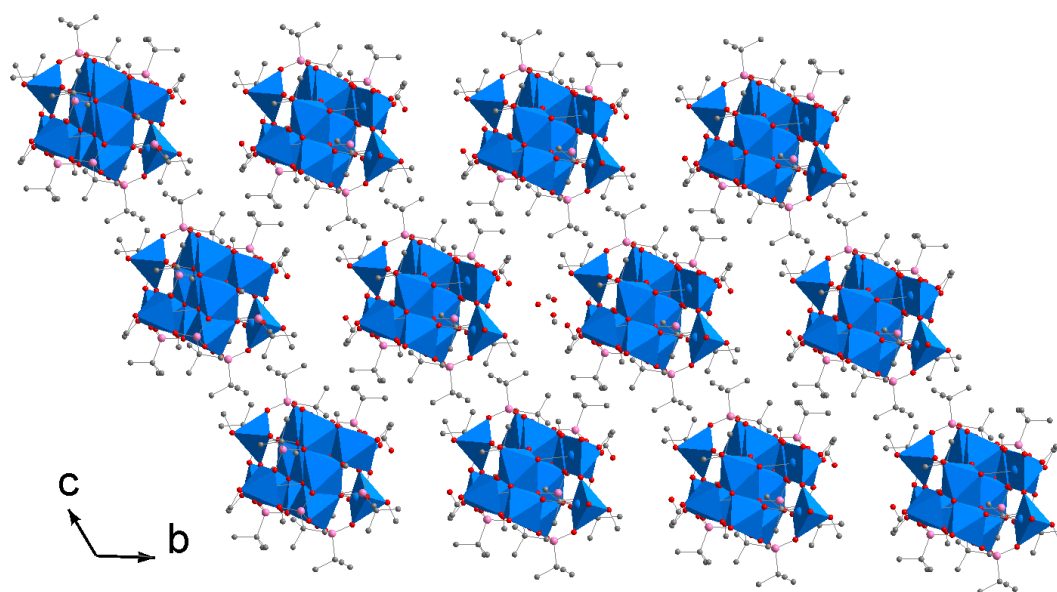


Figure S1. The packing structure of $[1]Cl_{0.5} \cdot 6CH_3OH$, with the Mn coordination geometries highlighted in polyhedral model. View in the direction of the crystallographic a -axis. The hydrogen atoms and solvent molecules are omitted for clarity.

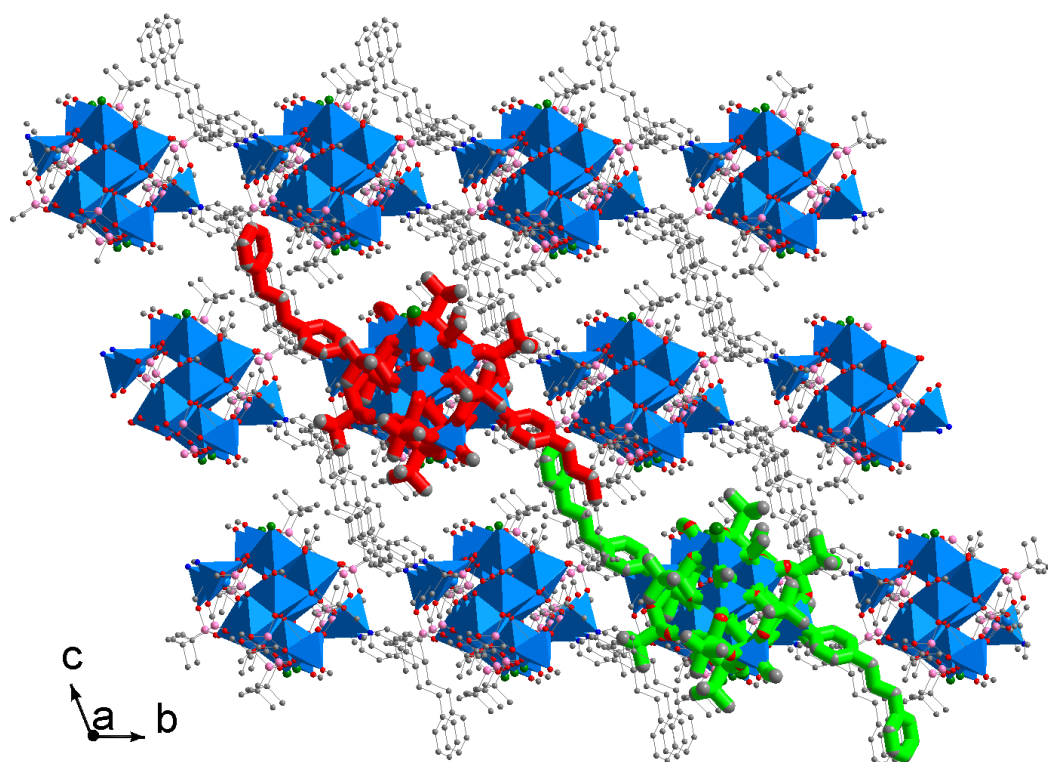


Figure S2. The packing structure of $[2] \cdot 1.5(\text{H}_3\text{O}) \cdot 8\text{CH}_3\text{OH}$, with the Mn coordination geometries highlighted in polyhedral model. View in the direction of the crystallographic a -axis. The hydrogen atoms and solvent molecules are omitted for clarity.

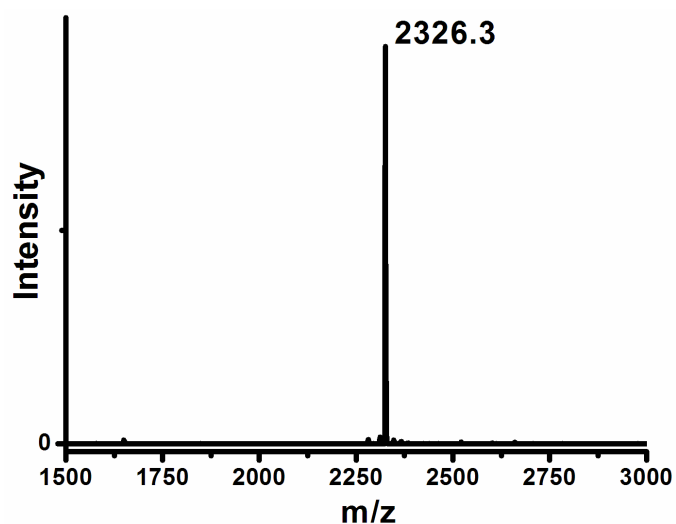


Figure S3. Negative-mode ESI-MS spectra of **2**: crystals dissolved in CH_3OH , the signal centered at m/z 2326.3 can be attributed to the corresponding $[\text{Mn}_{13}\text{O}_8(\text{CH}_3\text{O})_4(\text{tert}\text{-butyl-PO}_3)_{10}]^-$ species.

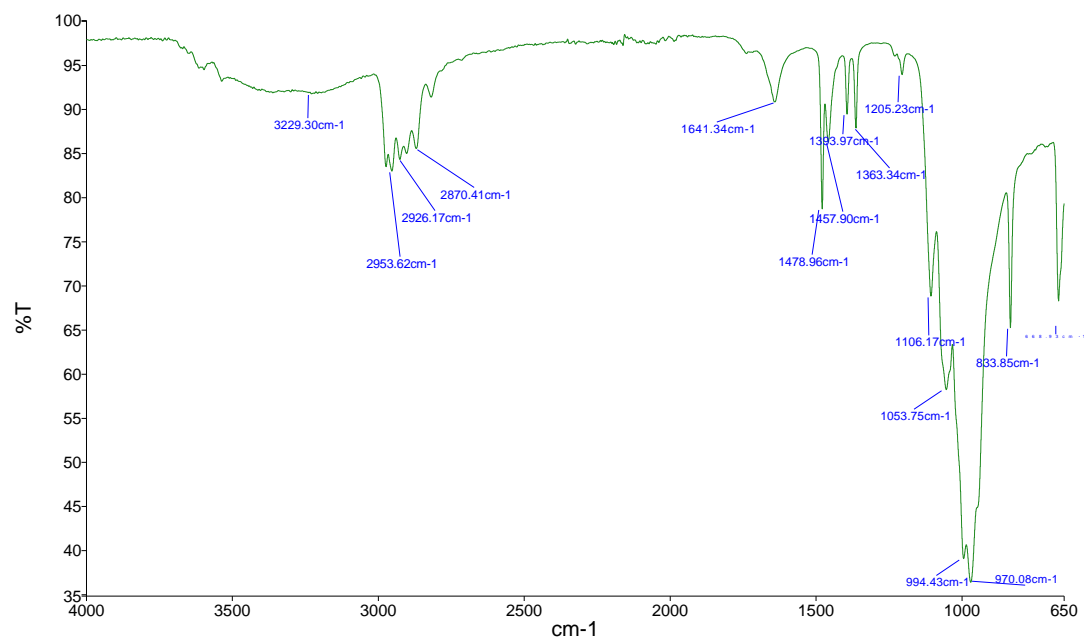


Figure S4. The IR spectrum of [1]Cl_{0.5}·6CH₃OH.

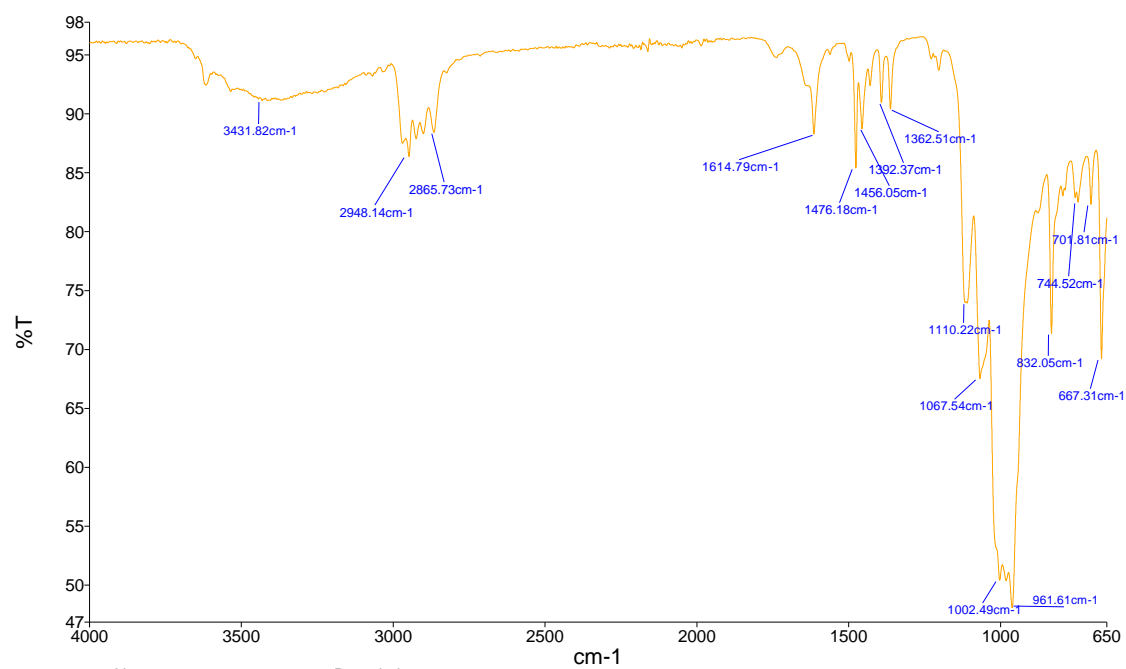


Figure S5. The IR spectrum of [2]·1.5(H₃O)·8CH₃OH.

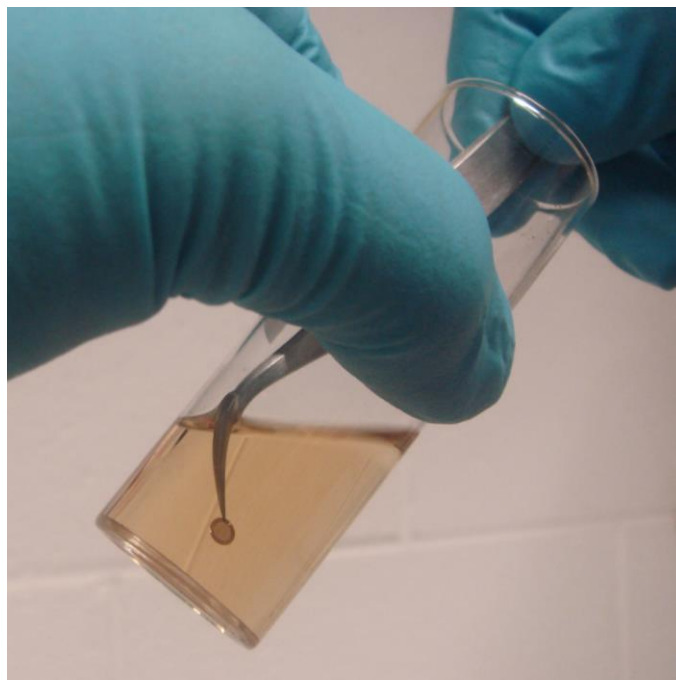


Figure S6. Photography of the films preparation.

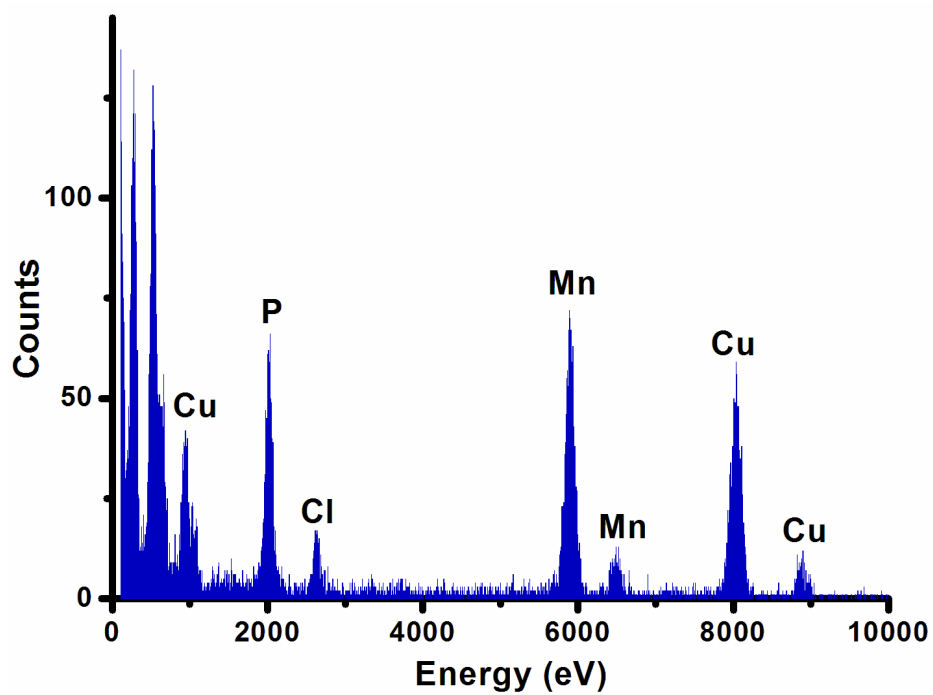
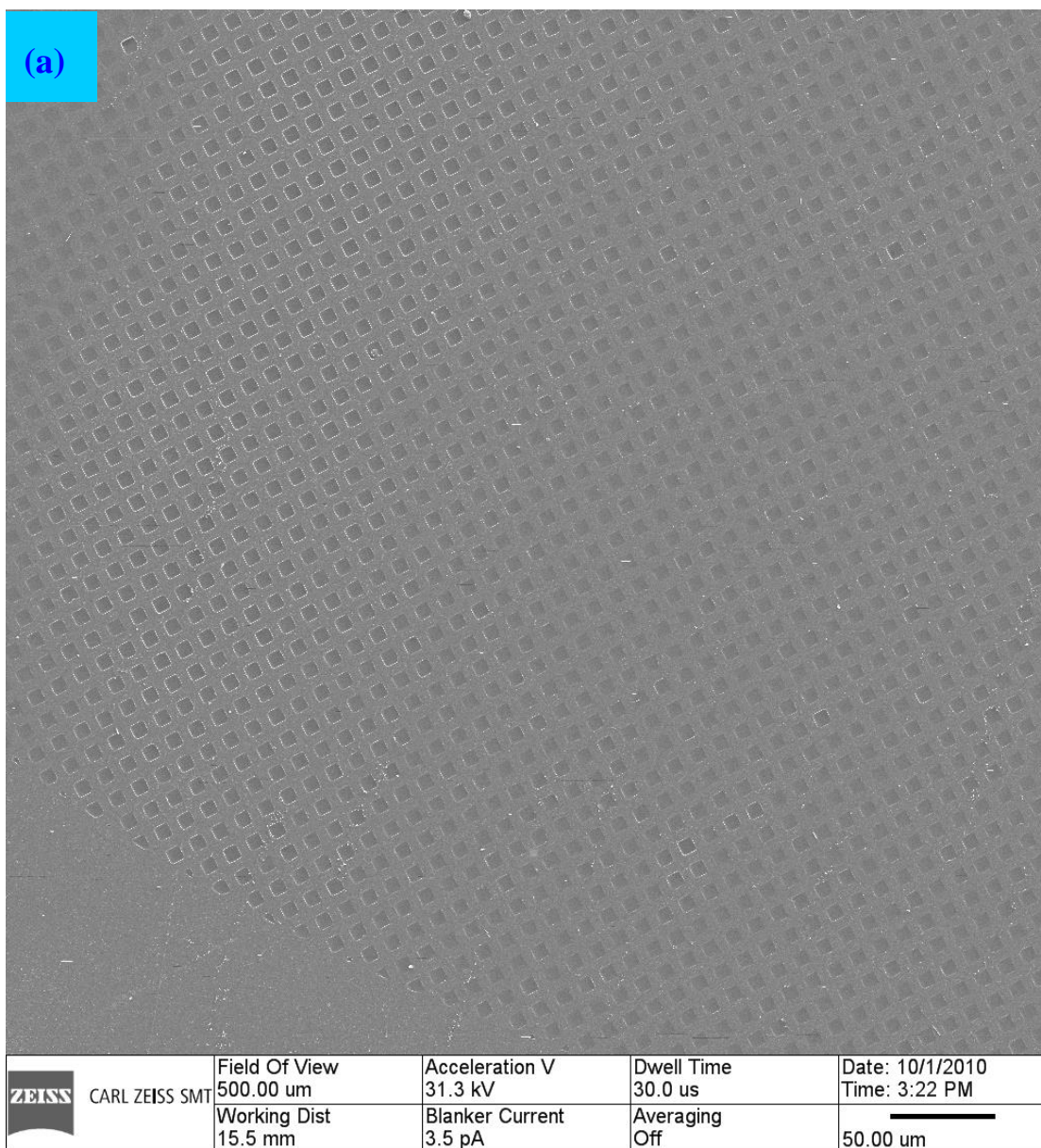
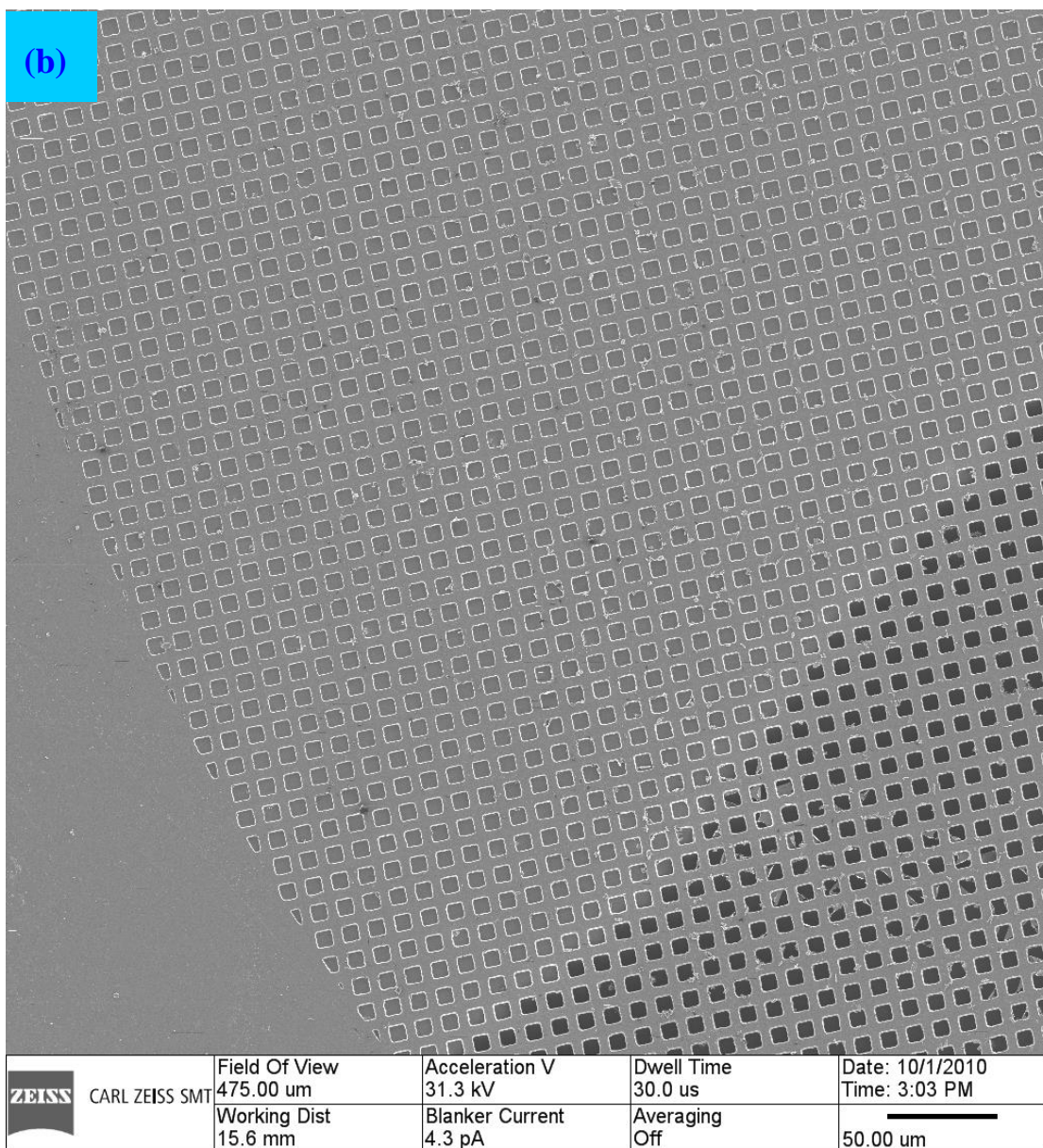
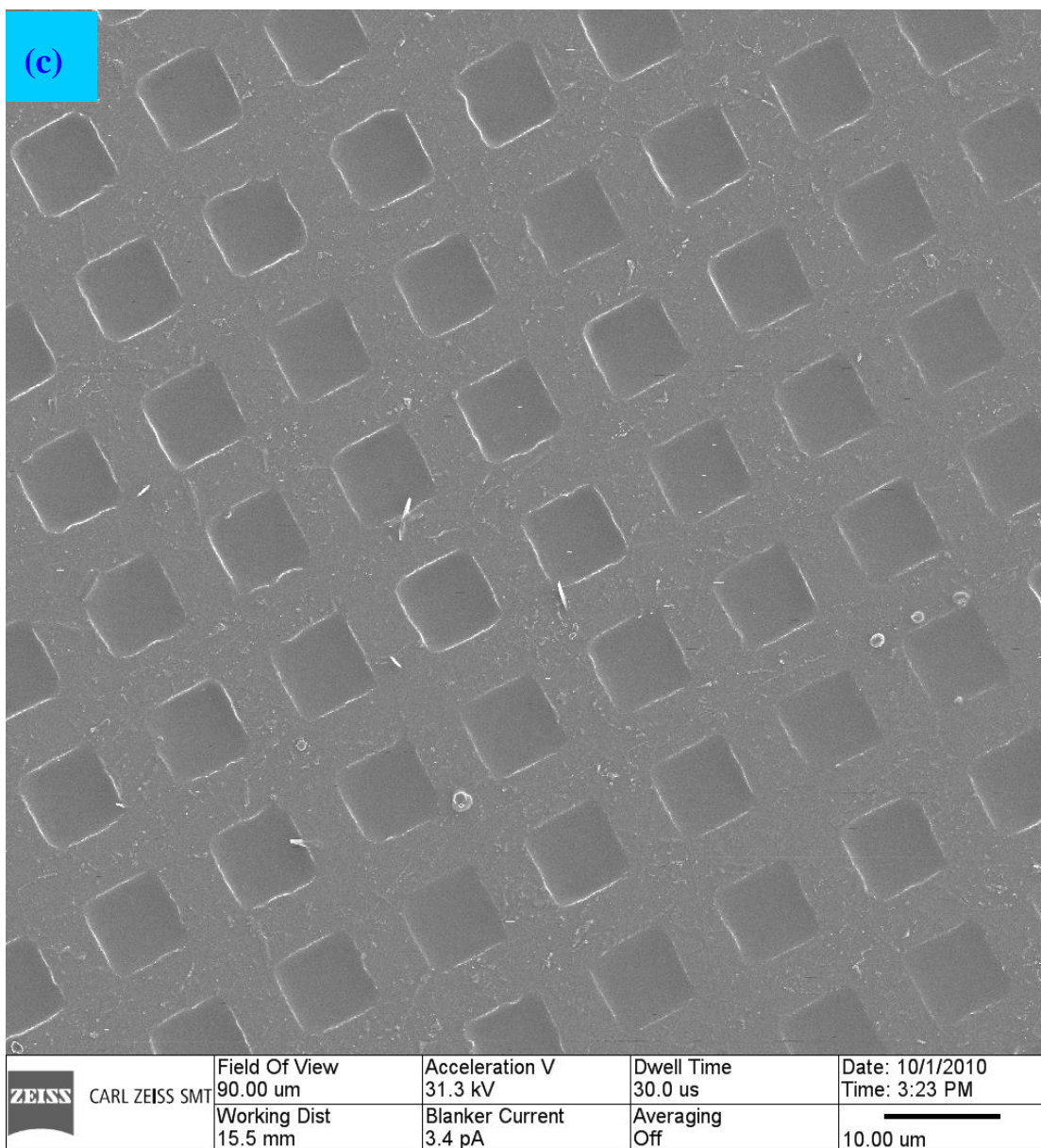


Figure S7. EDX analysis of the DFFs based on **2**.







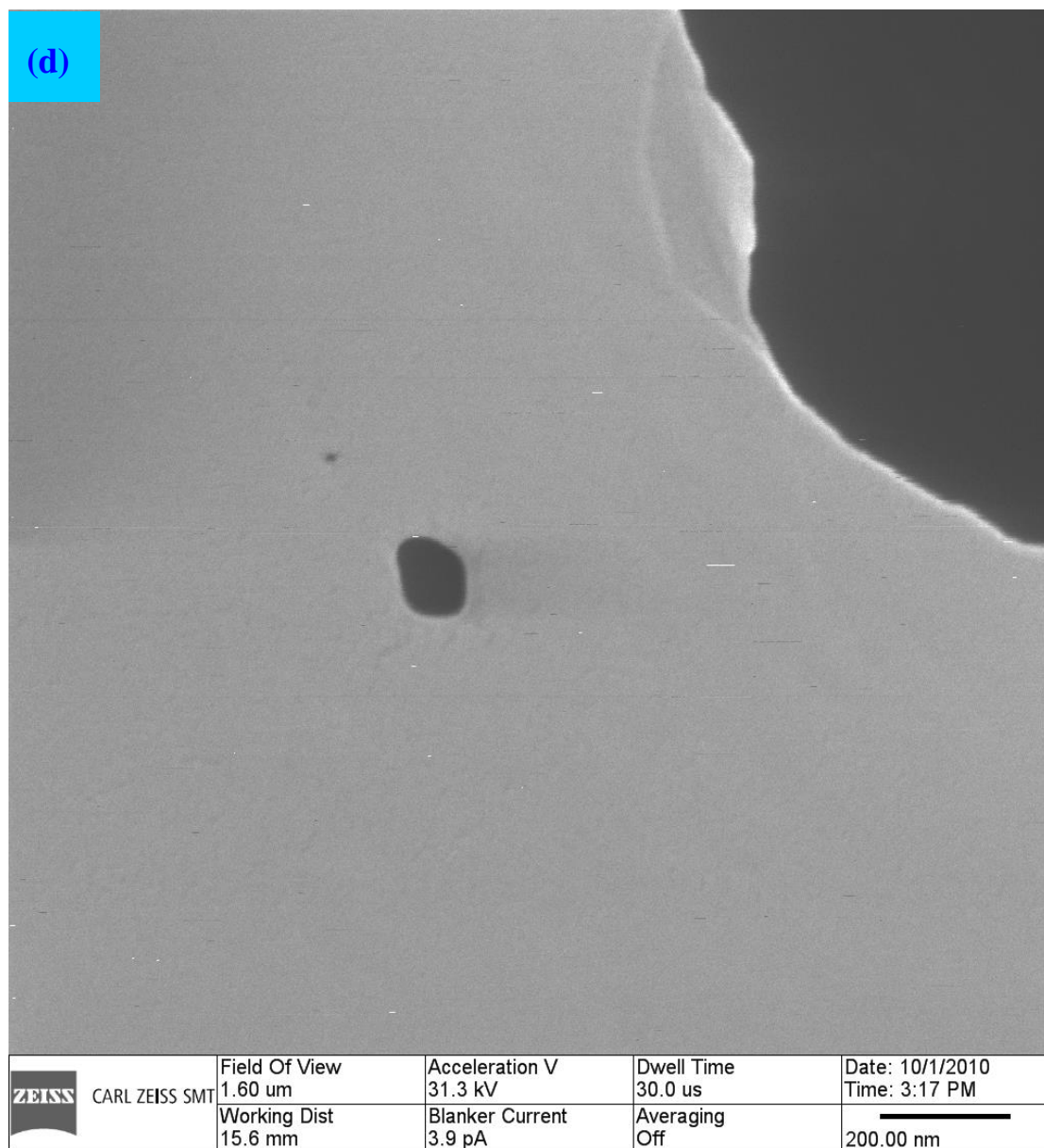
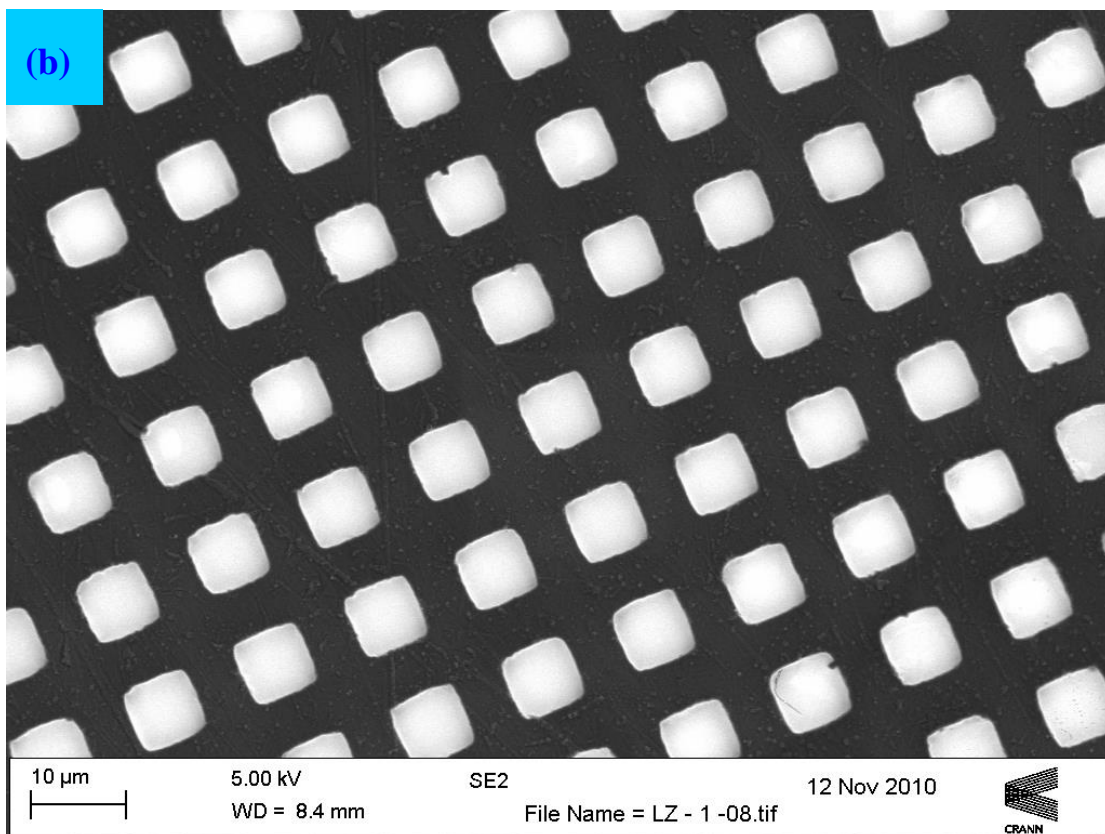
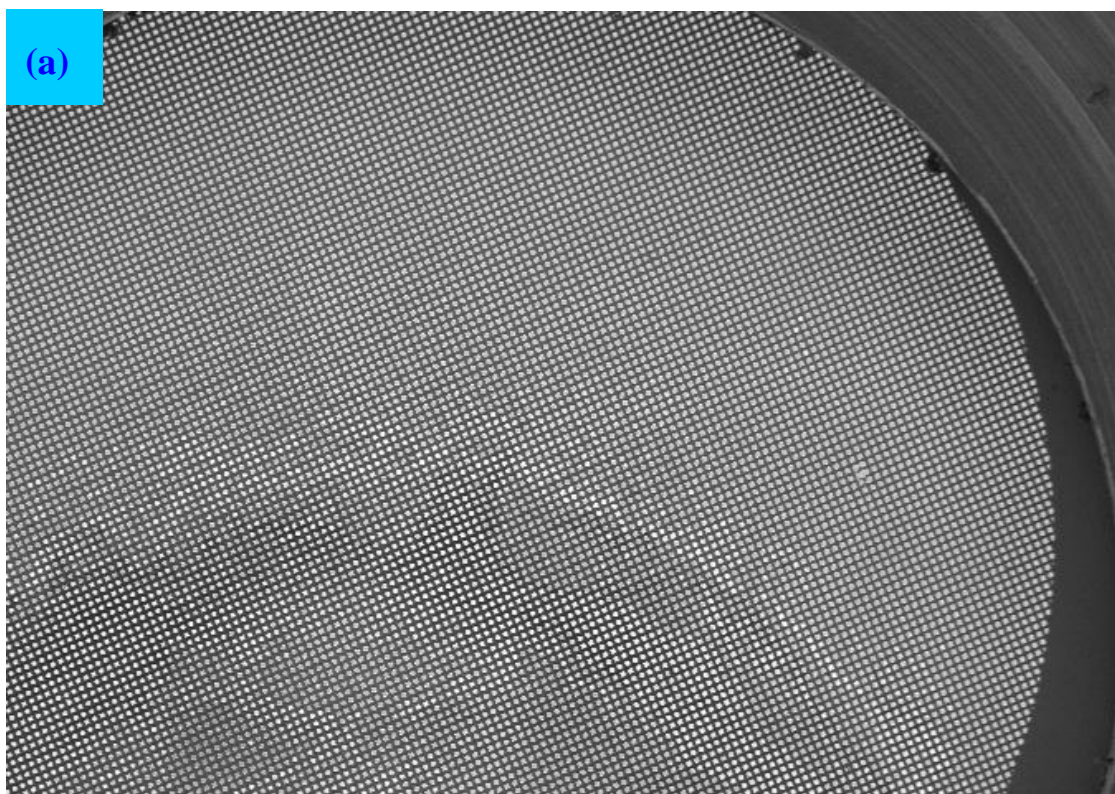


Figure S8. (a)–(d) HIM images of the DFFs of **2** (coated with a thin layer of Pt with a thickness about 5 nm) (preparative solution: 3 mg **[2]**·1.5(H₃O)·8CH₃OH in 10 ml MeOH). The middle hole in (d) was generated by the focused helium ion beam.



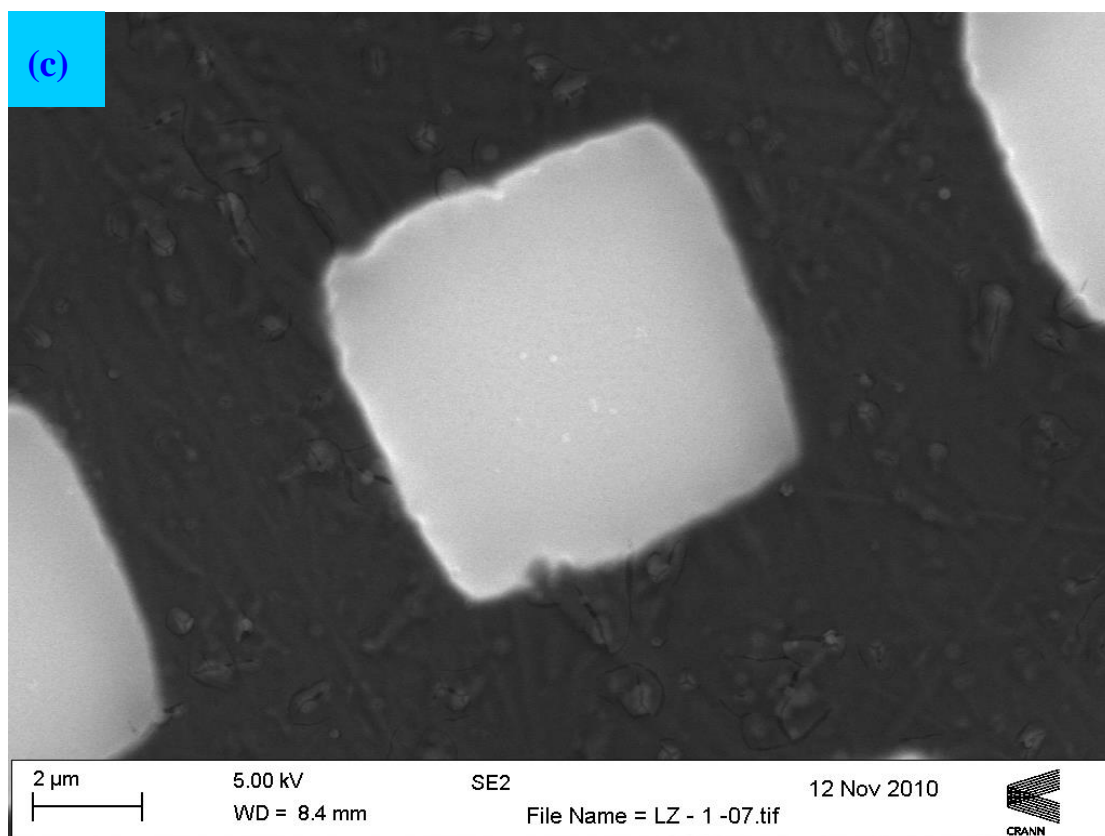
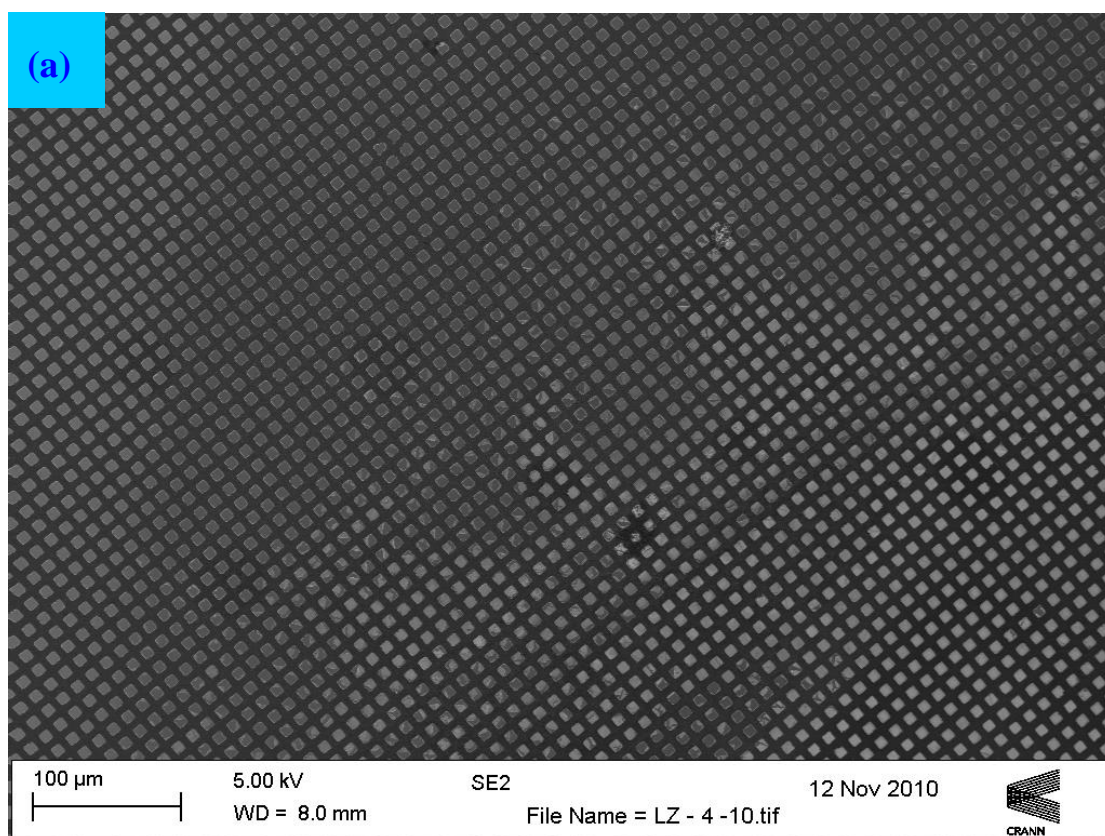
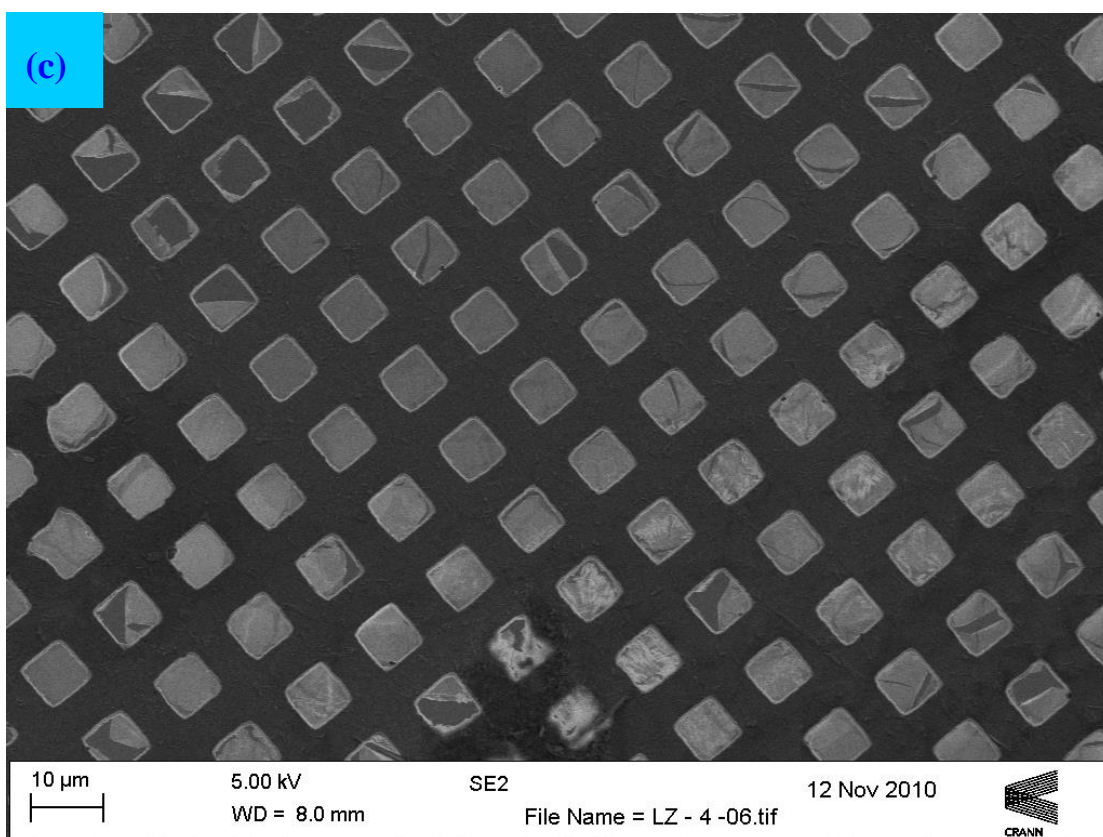
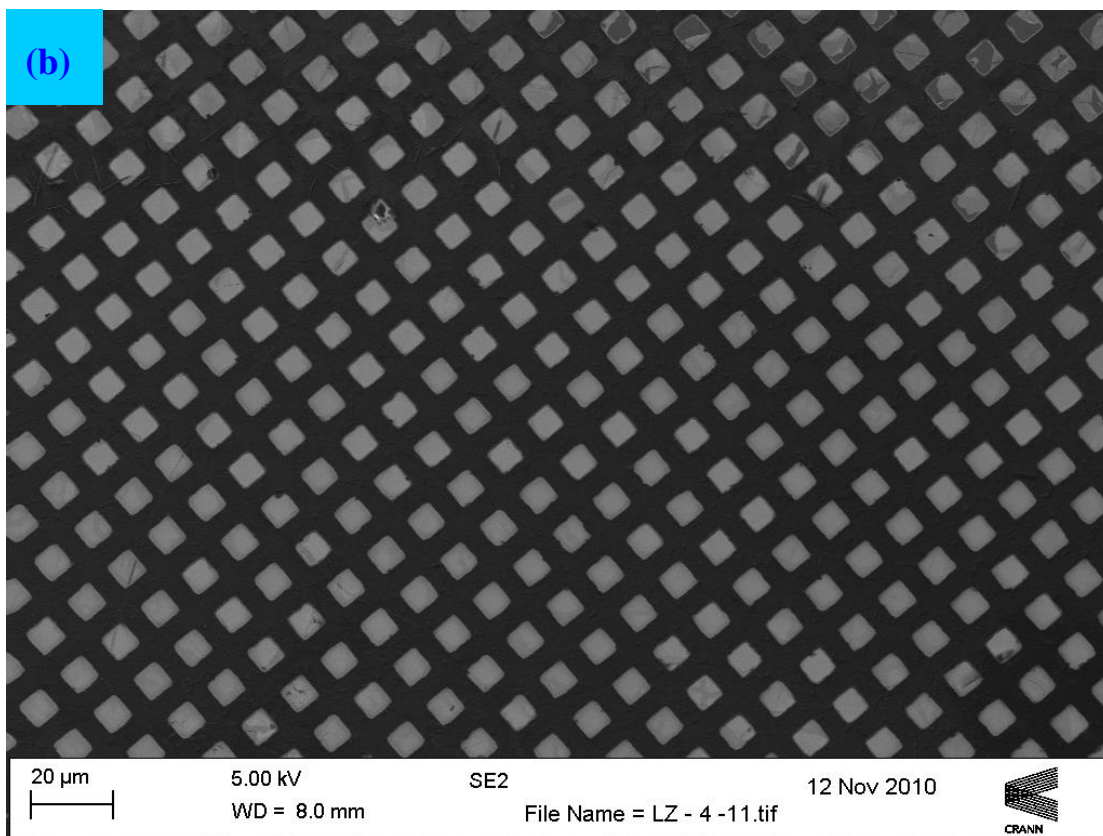
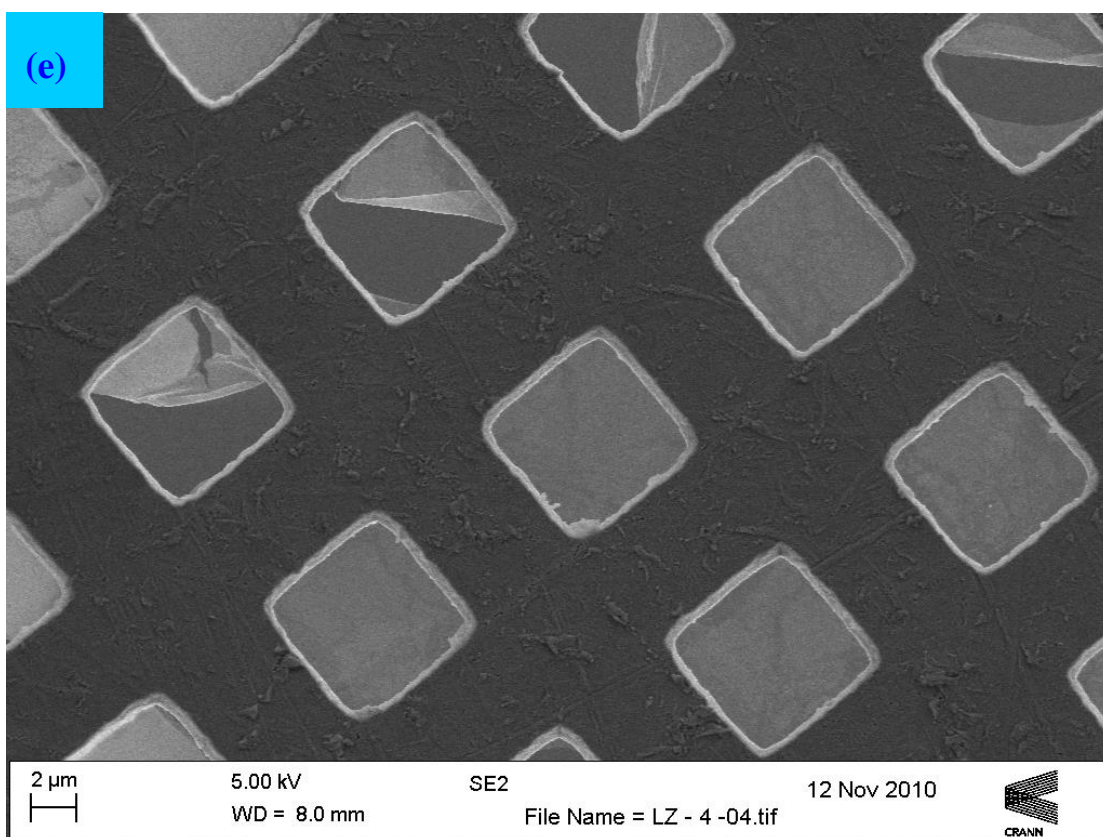
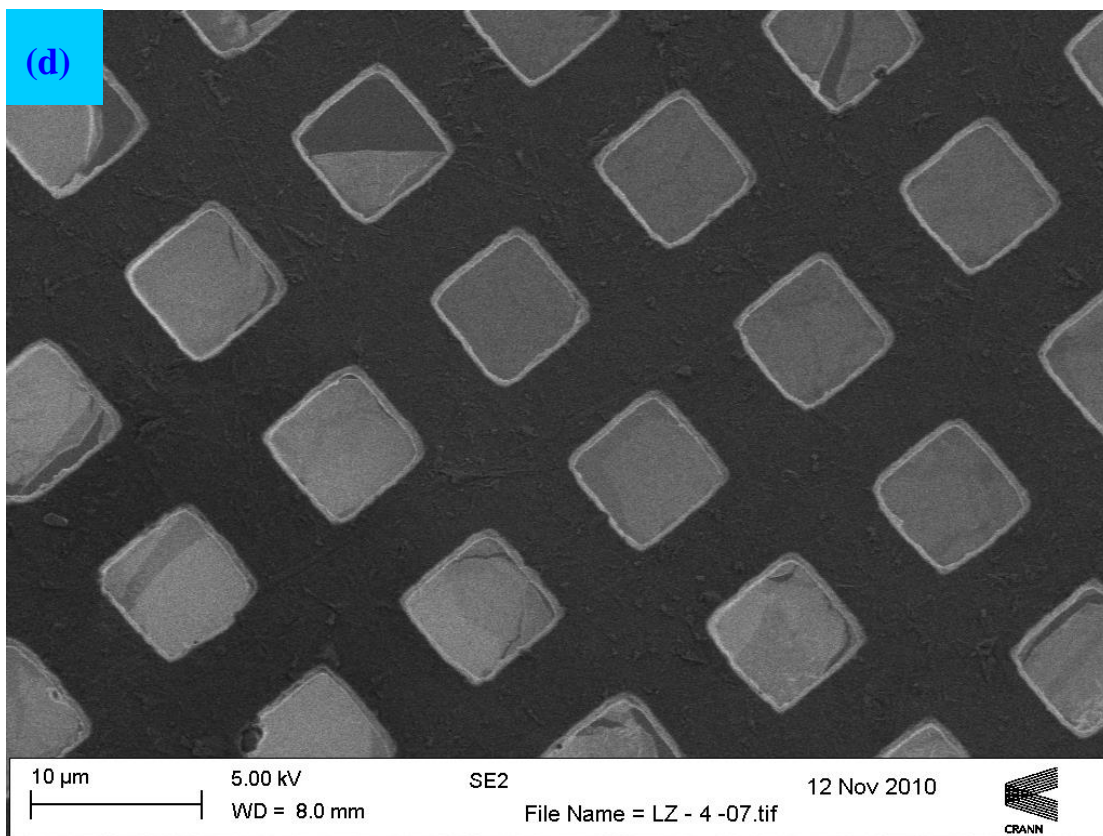


Figure S9. (a)–(c) SEM images of the DFFs of **2** (preparative solution: 3 mg **[2]**·1.5(H₃O)·8CH₃OH in 10 ml MeOH).







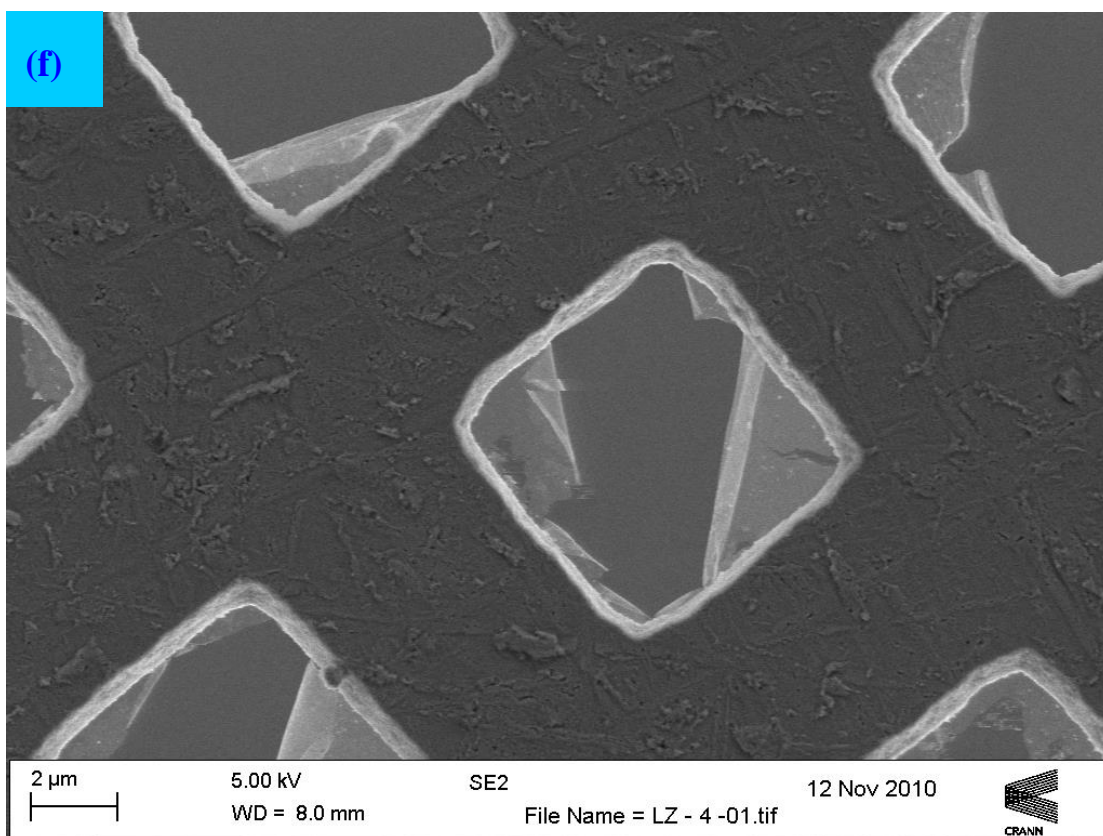
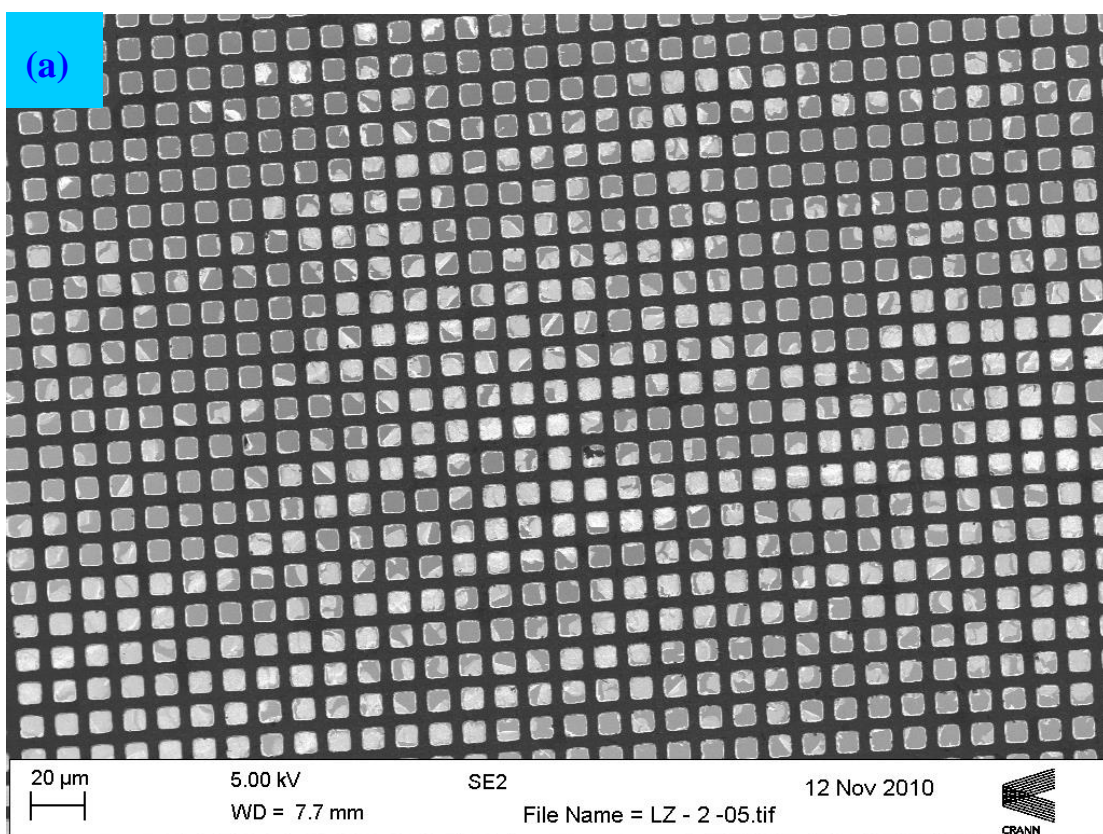


Figure S10. (a)–(f) SEM images of the DFFs of **2** (preparative solution: 1 mg [2]·1.5(H₃O)·8CH₃OH in 10 ml MeOH).



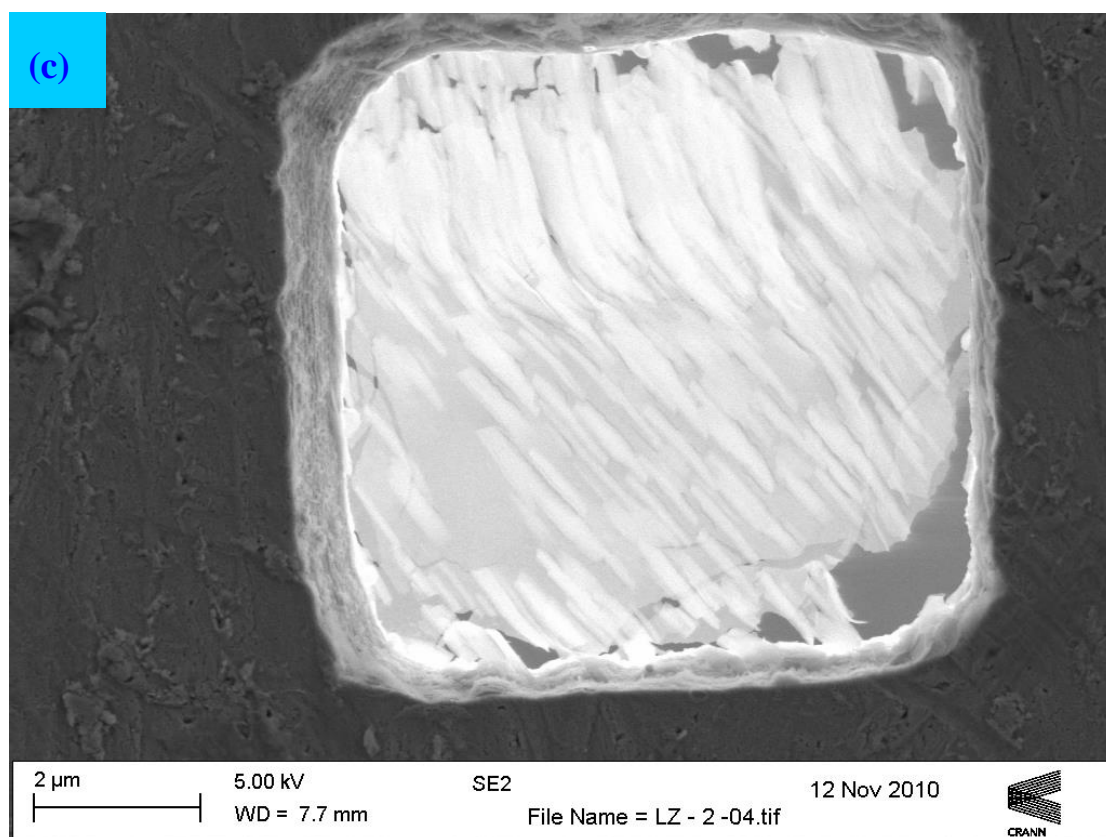
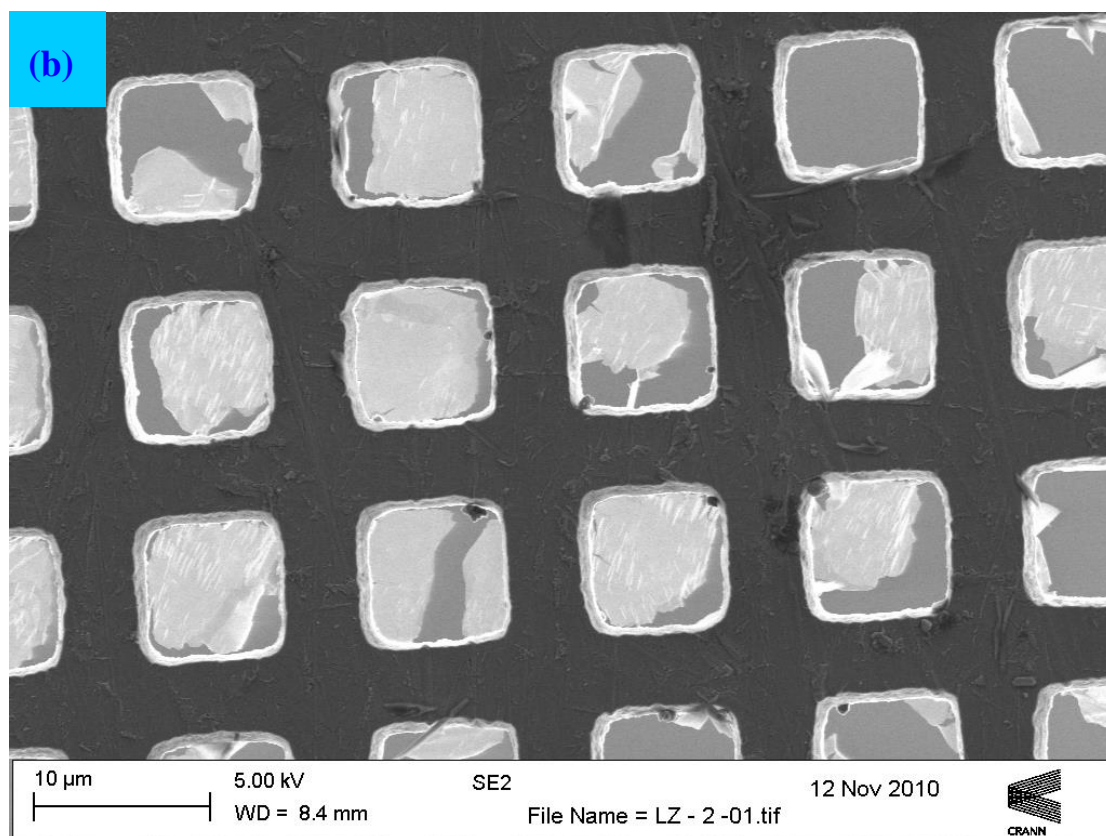
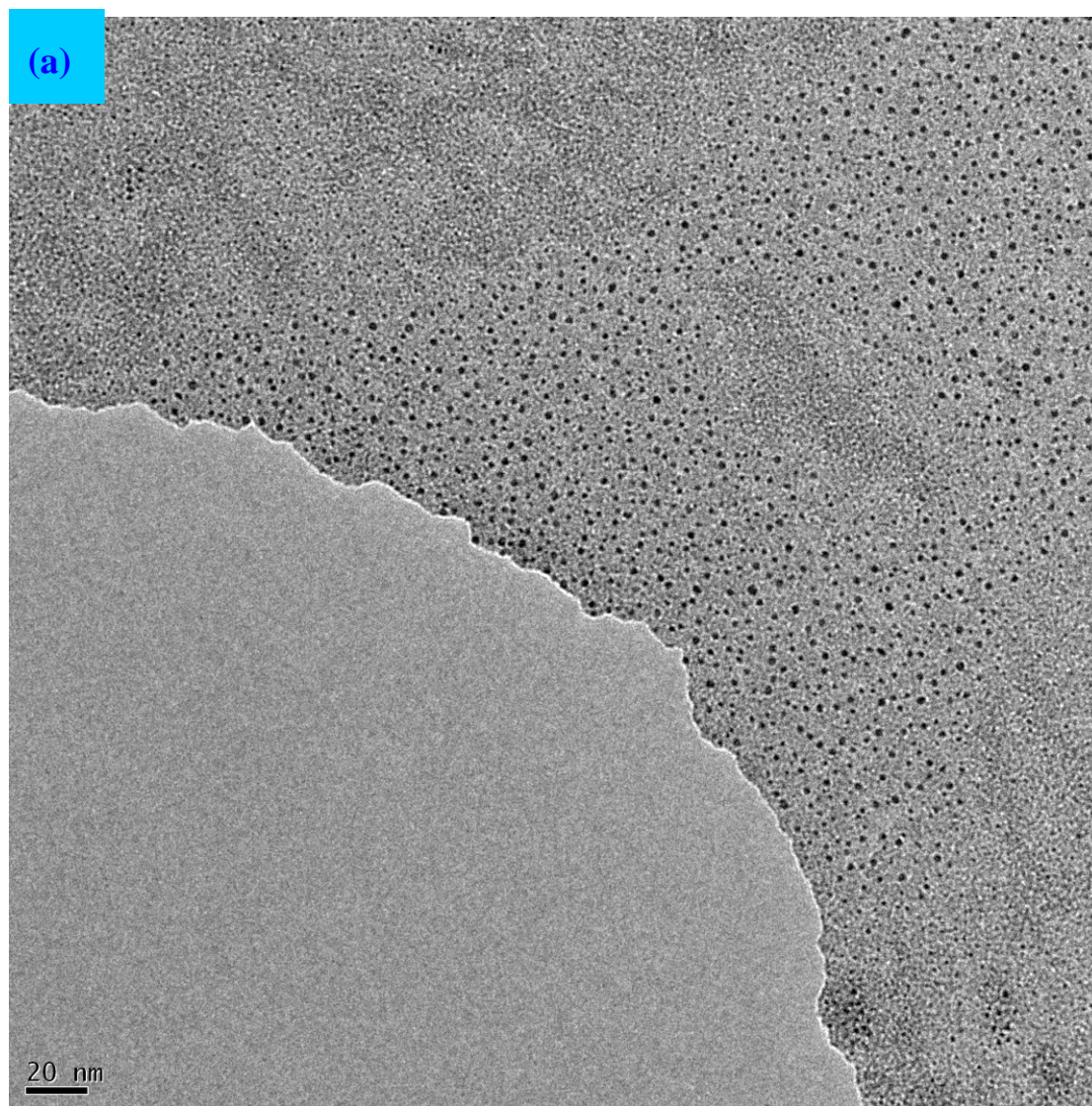
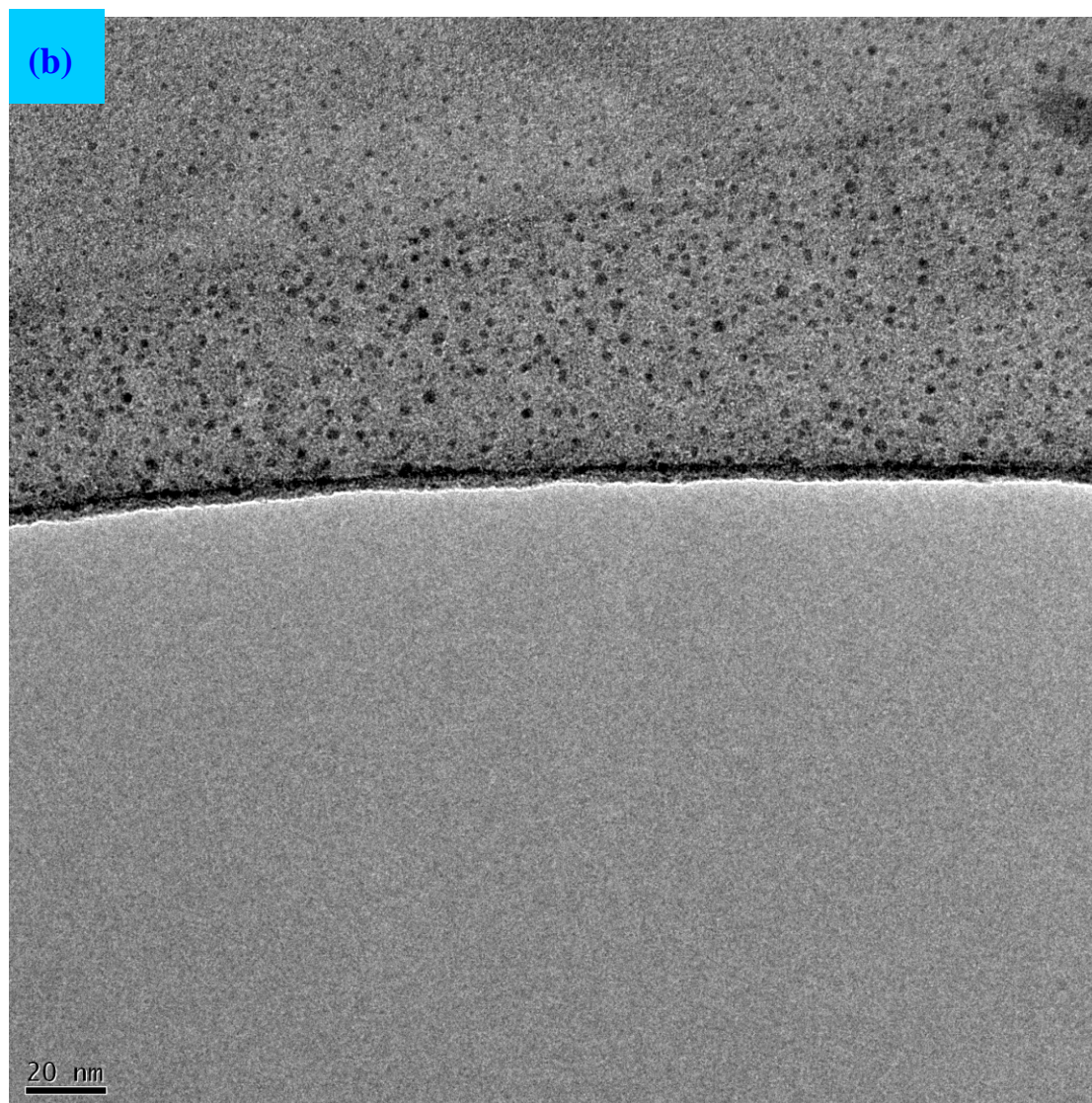
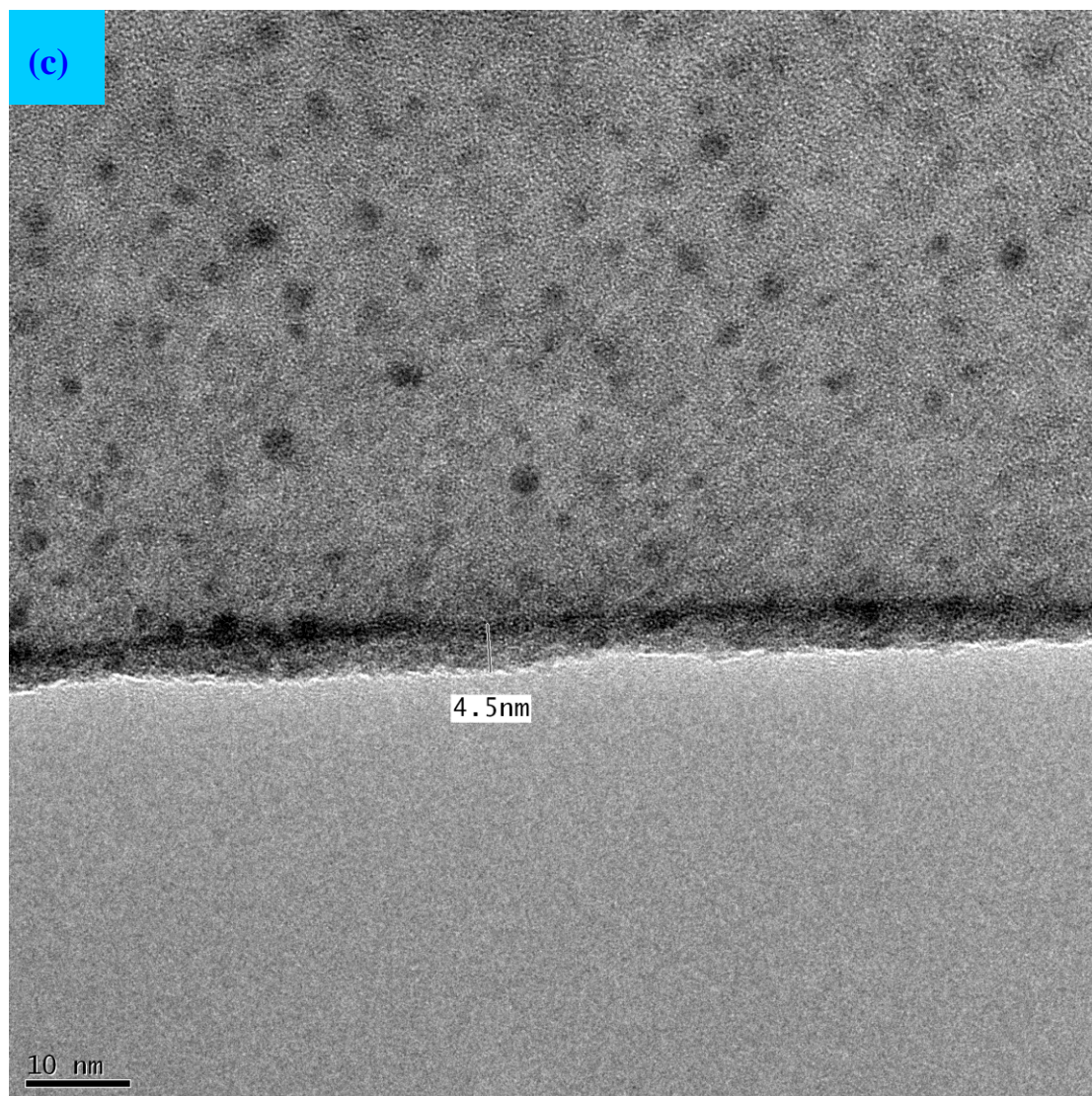
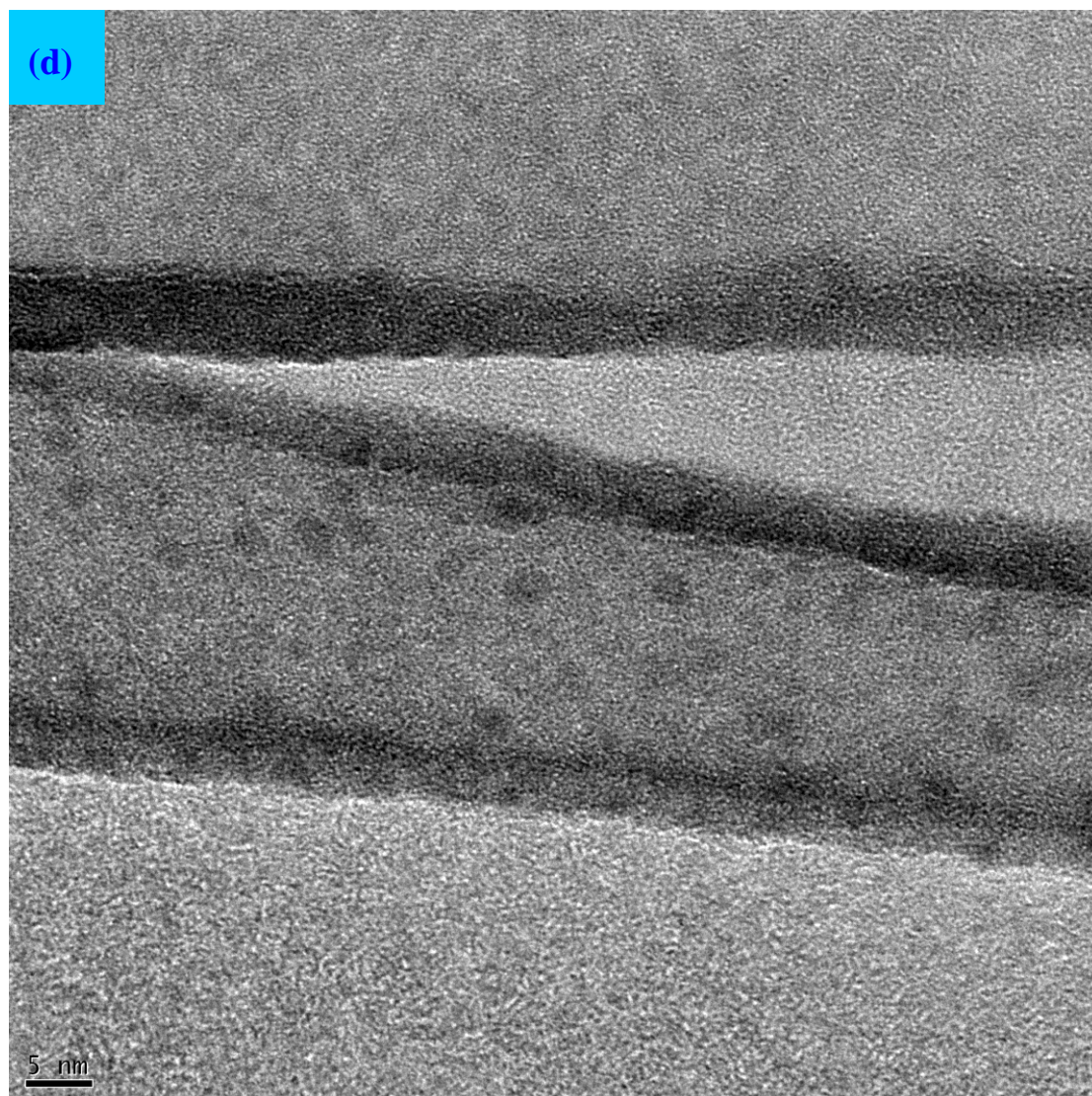


Figure S11. (a)–(c) SEM images of the DFFs of **2** (preparative solution: 3 mg **2**·1.5(H₂O)·8CH₃OH in 10 ml MeCN).









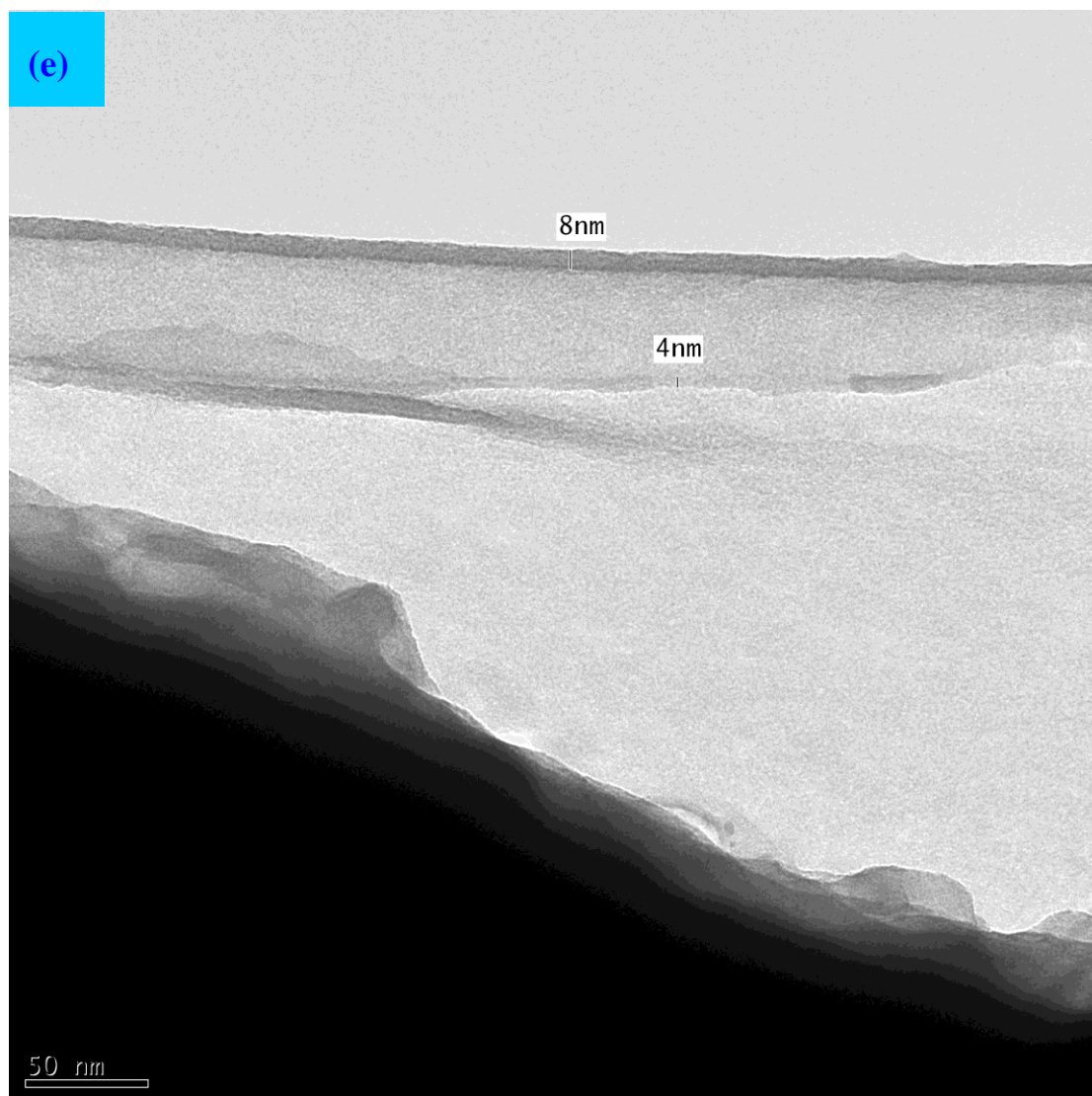
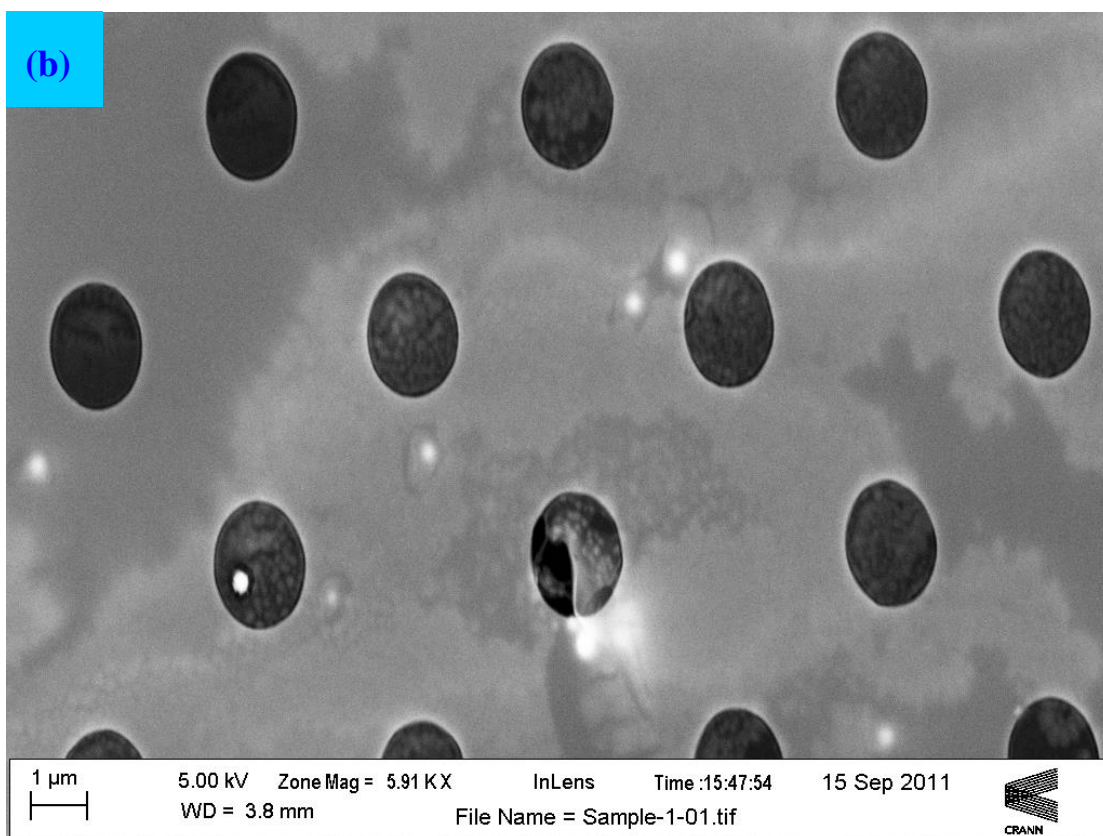
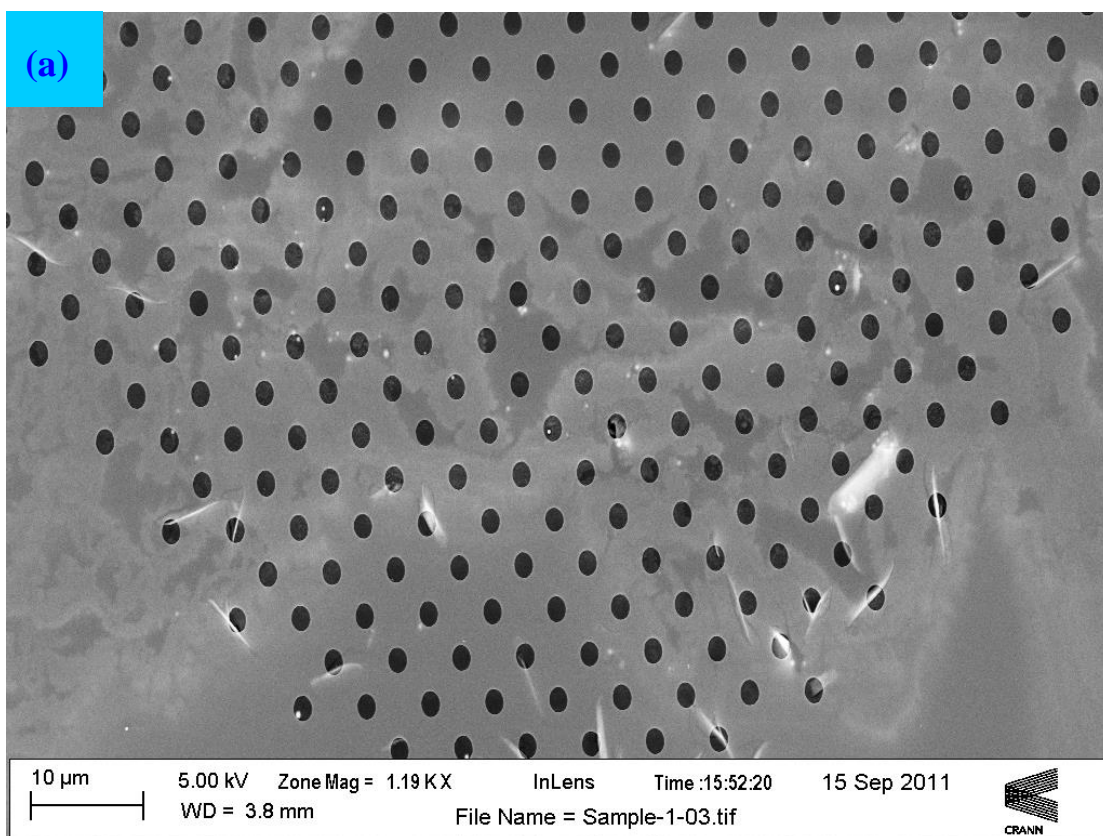


Figure S12. (a)–(e) TEM images of the DFFs of **2** (preparative solution: 3 mg **[2]**·1.5(H₃O)·8CH₃OH in 10 ml MeOH).



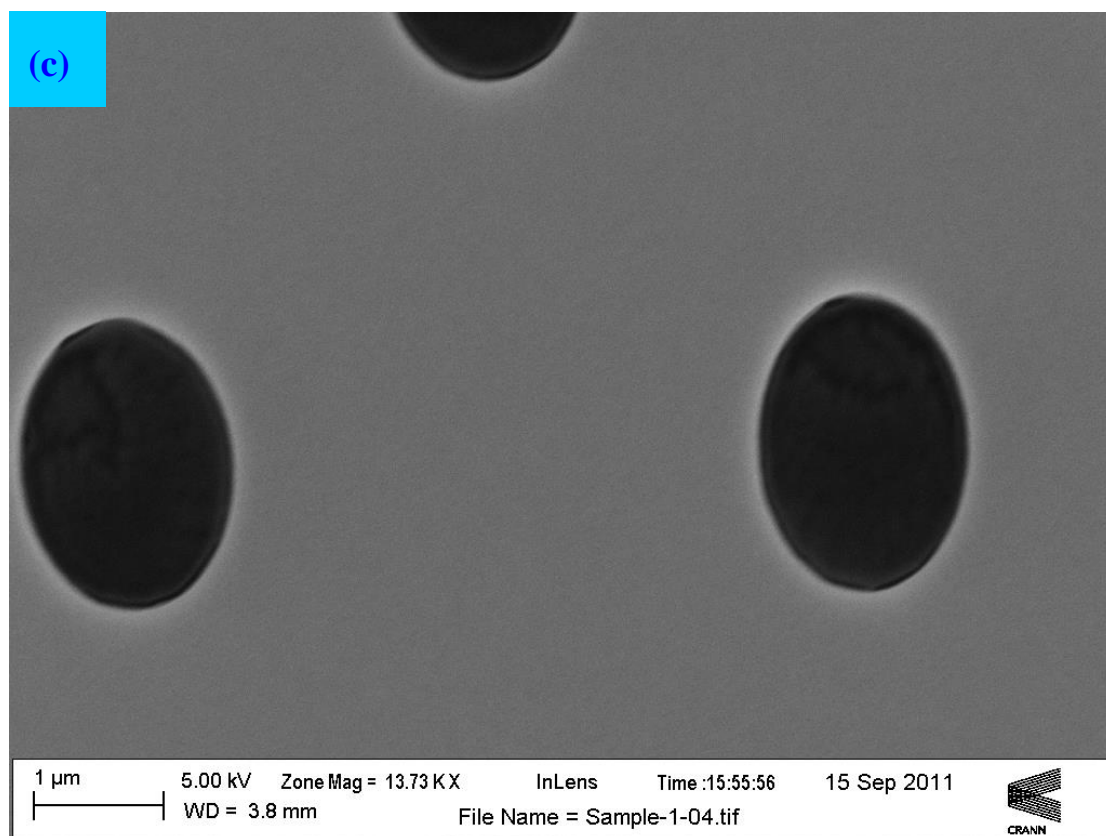


Figure S13. (a)–(c) SEM images of the DFFs of **2** (preparative solution: 3 mg [2]·1.5(H₃O)·8CH₃OH in 10 ml MeOH) with the Si₃N₄ grids composed of spherical holes.

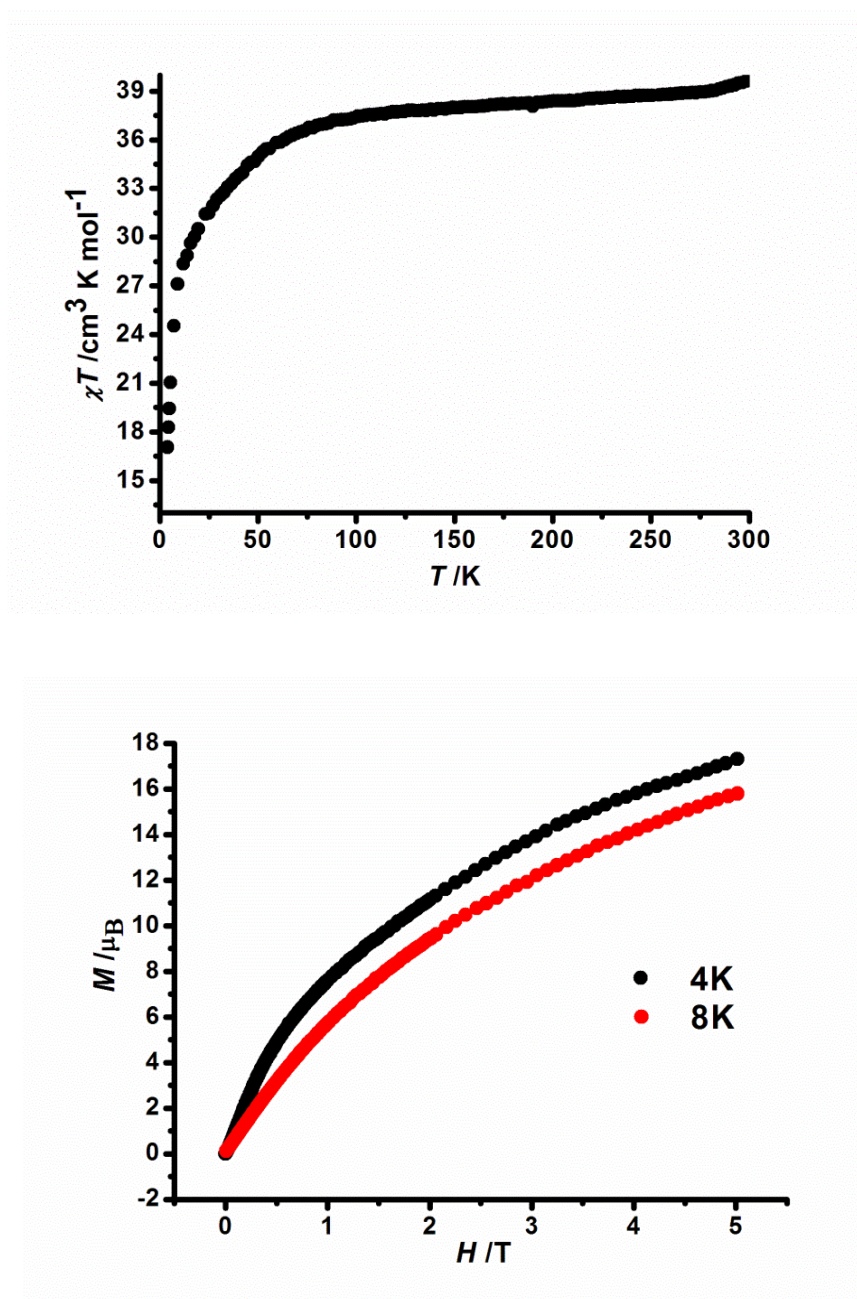


Figure S14. Magnetic properties at of $((\text{H}_3\text{O})_{1.5}[\mathbf{2}] \cdot 8\text{CH}_3\text{OH})$; *Top*: Temperature dependence of the χT product at 1000 Oe (χ is the molar magnetic susceptibility calculated from the ratio of the magnetization over the applied dc magnetic field, M/H , per complex); *Bottom*: Field-dependence of the magnetization. The measurements were performed using a Quantum Design MPMS-XL SQUID magnetometer using a freshly filtered sample (17.1 mg). The χT product at room temperature is in relative good agreement with the Curie constant expected ($39.7 \text{ cm}^3 \text{ K/mol}$) for $12.5 S = 3 \text{ Mn(III)}$ and $0.5 S = 5/2 \text{ Mn(II)}$ spins. The decrease of the χT product as well as the slow saturation of the M vs H data highlight the presence of dominating antiferromagnetic interactions in the complex.